Configuration Interaction Study of the Low-Lying Electronic States of Silicon Monoxide

Surya Chattopadhyaya, Anjan Chattopadhyay, and Kalyan Kumar Das*

Department of Chemistry, Physical Chemistry Section, Jadavpur University, Kolkata 700 032, India

Received: August 6, 2002; In Final Form: October 16, 2002

The electronic spectrum of the silicon monoxide molecule has been studied theoretically by using ab initio-based multireference singles and doubles configuration interaction calculations, which include the effective core potentials of the atoms. Potential energy curves of all 18 states, which correlate with the lowest dissociation limit $Si(^3P_g) + O(^3P_g)$, are constructed. Spectroscopic parameters, namely, T_e, r_e, and ω_e of a large number of bound Λ-S states of the molecule, are estimated and compared with the available experimental and other theoretical data. In addition, dissociation energies and dipole moments of the ground and some excited states are computed. The changes in the spectroscopic properties and potential energy curves after the inclusion of the spin−orbit coupling are discussed. Transition probabilities of many dipole-allowed and spin forbidden transitions are reported. The radiative lifetimes of some of the excited states such as $A^1\Pi$, $E^1\Sigma^+$, and $2^1\Pi$ are estimated and compared with the experimental results. Dipole moments (μ) and dipole derivatives ($\partial\mu/\partial r$) of the molecule in $X^1\Sigma^+$, $a^3\Sigma^+$, $b^3\Pi$, $A^1\Pi$, and $E^1\Sigma^+$ states as a function of the bond distance have been computed.

I. Introduction

The electronic structure and spectroscopic properties of silicon monoxide have been the subject of a number of experimental as well as theoretical investigations over the past several decades[1−36] for its astrophysical interest and its similarity to CO. The ultraviolet band system of SiO was first observed by Jevon[1] in the range of 2176.6−2925.3 Å. These bands are found to be due to a $^1\Pi - {}^1\Sigma^+$ transition analogous to the fourth positive band of CO.[2] The rotational analyses of these bands have been performed subsequently by Saper.[3] The Franck−Condon factor and *r*-centroids for some bands of the $A^1\Pi - X^1\Sigma^+$ system have been determined.[4] The absorption spectra of the gaseous SiO, GeO, and SnO in the region of 1250−2000 Å have been examined by Barrow and co-workers.[5,6] The vibrational analyses of a number of new band systems are also carried out by these authors. Spectroscopic constants of 11 states of SiO have been reported. Dissociation energies of some of these states have been determined. The linear extrapolation of vibrational levels of the ground state of SiO gives an approximate dissociation energy D_0 (SiO) ≃ 8.02 eV. The E state has been assumed to dissociate into $Si(^3P) + O(^3P)$ with an estimated dissociation energy of 1.53 ± 0.03 eV. In the region of 4200−4300 Å, a spectrum of $^1\Sigma^- - {}^3\Pi_r$ has been observed by Verma and Mulliken.[7] The lower $^3\Pi_r$ state of SiO is analogous to the $a^3\Pi_r$ state of CO with an electronic configuration of $\pi^4\sigma\pi$, while the upper state ($^1\Sigma^-$) of the present system is similar to $I^1\Sigma^-$ of CO with a configuration of $\pi^3\sigma^2\pi$. However, further studies of this spectrum have suggested that these bands involve a $^3\Sigma^- - {}^3\Pi$ transition instead of $^1\Sigma^- - {}^3\Pi$ as reported earlier.

Nair et al.[9] have calculated potential energy curves for some electronic states of oxides and sulfides of group IVA from the experimental energy levels by using some semiclassical method. Dissociation energies of these molecules are estimated from the potential curves. Two electronic transitions of SiO in the region of 3700−3950 Å and at 2970 Å have been observed[10,11] in a high-frequency discharge through a mixture of $SiCl_4$, oxygen, and argon flowing at low pressures. The vibrational as well as rotational analyses of the high-resolution spectrum have revealed two electronic transitions, namely, $c^3\Pi_i - a^3\Pi_r$ and $d^3\Sigma^+ - a^3\Pi_r$. It is also suggested that the upper state $d^3\Sigma^+$ is located 33 640 cm^{-1} above $a^3\Pi_r$. Bredohl et al.[12] have observed a spin forbidden transition $a^3\Pi_r - X^1\Sigma^+$ between 2870 and 3235 Å in emission using a hollow cathod discharge in flowing helium. The vibrational analysis of the a−X system has revealed two subbands, which correspond to $^3\Pi_1 - {}^1\Sigma^+_{0^+}$ and $^3\Pi_{0^+} - {}^1\Sigma^+_{0^+}$ components. The former transition is found to be more intense than the latter. These studies have determined spectroscopic constants of both $^3\Pi_1$ and $^3\Pi_{0^+}$ components. The dissociation energy of the $a^3\Pi_r$ state has also been reported.

Hager et al.[13] have studied the reaction $Si(^3P) + N_2O \rightarrow SiO + N_2$ in the gas phase. The emission spectrum of SiO has been assigned to two transitions, namely, $a^3\Sigma^+ \rightarrow X^1\Sigma^+$ and $b^3\Pi \rightarrow X^1\Sigma^+$. Because a new lowest $^3\Sigma^+$ state has been observed, these authors have designated $a^3\Pi_r$ as $b^3\Pi_r$. The reported T_0 values for a → X and b → X systems are 33 417 and 33 863 cm^{-1}, respectively. Verma and Shanker[14] have excited the emission bands of the $d^3\Pi_i - b^3\Pi_r$ system in a chemiluminescent flame of SiO. The rotational analysis and the deperturbation for the 0-1 band of the d−b system have revealed that the $d^3\Pi$ ($v = 0$) level is perturbed by the $A^1\Pi$ ($v = 23$) level. As a result of the mixing of $A^1\Pi$ with $d^3\Pi$, the (23-1) band of the $A^1\Pi - b^3\Pi_r$ transition has been observed.

During the search of triplet transitions of SiO, a simple Σ−Σ transition was observed in emission as a byproduct and attributed errorneously to the $B^2\Sigma^+ - X^2\Sigma^+$ transition of the SiO^+ ion.[15] Later on, Bredohl et al.[16] tentatively assigned this band system to a $^1\Sigma^- - {}^1\Sigma^-$ transition of neutral SiO. Barrow and Stone[17] have reinvestigated this band and identified it as the $E^1\Sigma^+ - X^1\Sigma^+$ system of SiO. The high-resolution absorption spectrum of $Si^{18}O$ has been recorded in the ultraviolet region to study many high-lying Rydberg states.[18,19] The ionization potentials of several states are also reported in these studies. Hager et al.[20] have observed the chemiluminescence spectrum of SiO produced in a flowing gas phase reaction $Si(^3P) + N_2O \rightarrow SiO + N_2$.

* To whom correspondence should be addressed. E-mail: kalyankd@hotmail.com, kalyankd@vsnl.net, das_kalyank@yahoo.com.

10.1021/jp021845v CCC: $25.00
Published on Web 12/06/2002

The emission bands are found to originate in the $b^3\Pi$ and $a^3\Sigma^+$ states and terminate in the ground state of SiO. These band systems are thus analogous to the spin forbidden Cameron $a^3\Pi-X^1\Sigma^+$ and the Hopfield−Birge $a^3\Sigma^+-X^1\Sigma^+$ systems of CO. A general survey has been made for the emission spectrum of the chemiluminescent flame of SiO, and the various band systems in the region of 2300−4600 Å have been identified by Shanker et al.[21] Linton and Capelle[22] have also investigated spectra of the chemiluminescent flame produced by the same reaction of silicon vapor with N_2O as mentioned above and observed strong emission from the $A^1\Pi-X^1\Sigma^+$, $b^3\Pi-X^1\Sigma^+$, and $a^3\Sigma^+-X^1\Sigma^+$ systems of SiO with a preferential excitation into the $b^3\Pi$ state.

Mass spectrometric determination[23] of the dissociation energy of gaseous SiO has been made by studying isomolecular equilibrium $Ge(g) + SiO(g) = GeO(g) + Si(g)$. The dissociation energy and ionization potential of SiO are reported to be 7.93 ± 0.13 and 11.6 ± 0.2 eV, respectively. However, an average of the dissociation energies obtained from several thermochemical determinations gives D_0^0 (SiO) = 8.26 eV.[24] The molecular beam electric resonance spectra of SiO and GeO have been measured by Raymonda et al.[25] to determine the electric dipole moments and dipole derivatives of these molecules in the lower vibrational states. In addition to a large number of experimental studies on the electronic states of SiO, there are many theoretical calculations as well.

McLean and Yoshimine[26] were the first to attempt the near Hartree−Fock ground state calculations of SiO. Later on, ab initio-based configuration interaction (CI) calculations on valence-excited states of SiO were performed by Heil and Schaefer.[27] Potential energy curves and spectroscopic constants of a large number of states, which dissociate into several low-lying limits, were also calculated by these authors. Oddershede and Elander[28] calculated spectroscopic constants and radiative lifetimes for valence-excited bound states in SiO by using the self-consistent polarization propagator approximation. Langhoff and Arnold[29] computed potential energy curves and some one electron properties for the $X^1\Sigma^+$, $C^1\Sigma^-$, $A^1\Pi$, and $E^1\Sigma^+$ states of SiO by using the self-consistent field (SCF) + CI method. These authors calculated a ground state dissociation energy of 8.1 eV. The electric dipole moment function (EDMF) for the ground state has been constructed. Transition probabilities and lifetimes for $A^1\Pi-X^1\Sigma^+$ and $E^1\Sigma^+-X^1\Sigma^+$ band systems are also reported. Werner et al.[30] have used MCSCF−CI wave functions with large basis sets to calculate potential energies and dipole moment functions for the ground state of SiO and for the $X\ ^2\Sigma^+$ and $A^2\Pi$ states of SiO^+. On the basis of the highly correlated ab initio calculations using the coupled electron pair approximation, Botschwina and Rosmus[31] studied spectroscopic properties of SiO and $HOSi^+$. Peterson and Claude Woods[32] performed singles and doubles CI to calculate potential energy and dipole moment functions for a large number of diatomics, which are isoelectronic with SiO. The most extensive study of EDMF of the SiO molecule was carried out by Tipping and Chackerian.[33] These authors also reported many transitions based on a dipole moment in the form of a Padé approximant chosen to reproduce the experimental moments for $v = 0-3$. Dipole moments of the oxides and sulfides of Si, Ge, Sn, and Pb were calculated by Kellö and Sadlej[34] using a variety of high-level correlated methods. These authors also determined the relativistic contributions to the dipole moment of these molecules in their ground state. The relativistic effect to the dipole moment was found to be negligibly small for SiO. Following this, Langhoff and Bauschlicher Jr.[35] computed an accurate EDMF for the SiO molecule by using large one particle basis sets and extensive treatment of the electron correlation. Very recently,[36] finite field many-body perturbation theory and coupled cluster calculations were used to accurately determine the electric dipole, the quadrupole moment, and the dipole polarizability of CS, SiO, and SiS molecules. In recent years,[37−41] ab initio-based CI calculations of the low-lying excited states of isovalent molecules such as GeS, GeSe, GeTe, and SiS were carried out to reveal their spectroscopic features. CI calculations of heavy molecules and clusters were extensively reviewed by Balasubramanian.[42,43]

In this paper, we have computed potential energy curves and spectroscopic features of low-lying electronic states of SiO by using the MRDCI method, which includes relativistic effective core potentials (RECP). The spin−orbit interactions are also introduced in the calculation to study spin forbidden transitions. The estimation of radiative lifetimes of some excited states of SiO is also the subject of the present study.

II. Methodology of Calculations

The core electrons of both Si and O were described by the effective potentials of Pacios and Christiansen.[44] As a result, $3s^23p^2$ electrons of Si and $2s^22p^4$ electrons of O were kept in the valence space for CI calculations. The total number of active electrons to be excited in the CI step was 10. The (4s4p) primitive Gaussian basis sets of Si were also taken from Pacios and Christiansen.[44] These were augmented with many diffuse and polarization functions. Three s functions (ζ_s = 0.04525, 0.02715, and 0.0163 a_0^{-2}), two p functions (ζ_p = 0.06911 and 0.02499 a_0^{-2}), five d functions (ζ_d = 4.04168, 1.46155, 0.52852, 0.19112, and 0.06911 a_0^{-2}), and two f type functions (ζ_f = 0.19112 and 0.06911 a_0^{-2}) were added.[45] The first two sets of d functions were contracted with contraction coefficients of 0.054268 and 0.06973, respectively.[45] Two sets of f functions were also contracted with coefficients 0.29301 and 0.536102, respectively.[45] Hence, the final AO basis set for Si in the present calculation was (7s6p5d2f/7s6p4d1f). For the oxygen atom, the (4s4p) basis set of Pacios and Christiansen[44] was augmented with a set of d functions of an exponent 1.33 a_0^{-2}, which made the final basis (4s4p1d) in the uncontracted form.

SCF calculations were carried out at each internuclear separation by using the above-mentioned RECP and basis sets of Si and O. These generated symmetry-adapted optimized molecular orbitals (MO) that were used as one particle basis for CI calculations. The silicon atom was kept at the origin with oxygen along the +*z*-axis. The entire computations were carried out in C_{2v} to take advantage of the simplicity of the Abelion group direct product relationship.

The one electron basis used for CI often depends on the state for which SCF MO calculations are carried out. The $\sigma^2\pi^4\ ^1\Sigma^+$ is known to be the ground state of SiO. Sometimes the SCF MOs of the ground state may not be suitable for the calculation of the excited states, which have occupied π^* MOs. In such a situation, it is required to optimize π^* MOs in the SCF calculation. There are three other choices of states, namely, $\sigma\pi^4\pi^{*3}\Pi$, $\sigma^2\pi^3\pi^{*3}\Sigma^-$, and $\pi^4\pi^{*2}\ ^3\Sigma^-$, which could be used for SCF MO calculations. However, $\sigma\pi^4\pi^{*3}\Pi$ and $\sigma^2\pi^3\pi^{*3}\Sigma^-$ states have the disadvantage of having inequivalent π_x and π_y components, while the doubly excited $^3\Sigma^-$ state does not pose such a problem. Throughout the present calculations, eigenvalues and eigenfunctions retain their perfect symmetries in B_1 and B_2 irreducible representations. Hence, the Π states remain symmetry pure. The MRDCI codes of Buenker and coworkers[46−51] are used in the present study. In the first step, the calculations of Λ-S states were carried out by incorporating all

relativistic effects except the spin−orbit term through RECP. For the low-lying states of a given spatial and spin symmetry, a set of reference configurations were chosen for excitations. These reference configurations describe the states throughout the potential energy curves. All possible single and double excitations were permitted from each of these reference configurations. The eight lowest roots were optimized for states of singlet and triplet spin multiplicities, while five roots were computed for quintets. A large number of configurations, up to 15 million, were generated from these excitations. However, the configuration selection and energy extrapolation techniques were employed to reduce the sizes of the secular equations. In the present calculations, we have fixed the configuration selection threshold at 5.0 μhartree so that the largest dimension of the selected CI space remains below 50 000. The sum of the squares of coefficients of the reference configurations for each root always remained above 0.90. The effect of higher order excitations from these reference configurations was partially adjusted by the multireference analogue of the Davidson correction.[52,53] However, the correction did not make much difference in excitation energies. The estimated full CI energies and CI wave functions of Λ-S states were used for the calculations of spectroscopic and transition properties of the SiO molecule.

The spin−orbit coupling was included in the next step by employing the spin−orbit operators[44] compatible with RECP of Si and O. The spin-independent MRDCI wave functions were multiplied with appropriate spin functions, which transformed as C_{2v} irreducible representation. The Ω states obtained after the spin−orbit interaction were classified into A_1, A_2, and B_1 representations of C_{2v}^2. The B_2 representation was degenerate with B_1; hence, states belonging to B_2 were not computed. The full CI energies in the Λ-S CI calculations were kept in the diagonals of the Hamiltonian matrix, while the off-diagonal elements were calculated from the RECP-based spin−orbit operators and Λ-S CI wave functions. Energies and wave functions of spin−orbit states were obtained from the diagonalization of these spin−orbit blocks. All Λ-S states, which correlate with the lowest limit $Si(^3P_g) + O(^3P_g)$, were included in the spin−orbit CI treatment. The advantage in such a two step procedure for the inclusion of the spin−orbit coupling was that the wave functions of Ω states could be easily analyzed in terms of Λ-S eigenfunctions. Moreover, the computational labor was much lower to achieve the desired level of accuracy.

Potential energy curves of spin-independent and spin-included states of SnO were fitted into polynomials to determine their spectroscopic parameters. The nuclear Schrödinger equations were then solved numerically to compute vibrational energies and wave functions, which were used to calculate transition dipole moments for the pair of vibrational functions in a particular transition. Einstein sponteneous emission coefficients and transition probabilities were calculated. Finally, the radiative lifetimes of excited states at various vibrational levels were estimated from these data.

III. Results and Discussion

Λ-S Potential Energy Curves. Eighteen Λ-S states of singlet, triplet, and quintet spin multiplicities correlate with the ground states of both Si and O atoms. The first excited state (^1D_g) of Si interacts with the ground state of O to generate nine triplets, while the next higher state (^1S_g) of Si provides three states, namely, $^3\Sigma^-$ and $^3\Pi(2)$. Table 1 shows how the molecular states of SiO correlate with atomic states in the lowest dissociation limits along with their relative energies. The observed energy separation between ^3P_g and ^1D_g states of Si is nearly 1500 cm^{-1} smaller than the value computed from the MRDCI calculations of the molecule at a very large bond length ($r > 15$ a_0). Figure 1a−c shows the potential energy curves of the low-lying singlets, triplets, and quintets of SiO, respectively. All of the curves converge into the lowest dissociation limit $Si(^3P_g) + O(^3P_g)$. In Table 2, we have displayed spectroscopic constants

TABLE 1: Dissociation Correlation between the Molecular and the Atomic States of SiO

molecular state	atomic state Si + O	relative energy (cm^{-1}) expt[a]	relative energy (cm^{-1}) calcd
$^1\Sigma^+(2)$, $^1\Sigma^-$, $^1\Pi(2)$, $^1\Delta$, $^3\Sigma^+(2)$, $^3\Sigma^-$, $^3\Pi(2)$, $^3\Delta$, $^5\Sigma^+(2)$, $^5\Sigma^-$, $^5\Pi(2)$, $^5\Delta$	$(3p^2)^3P_g + (2p^4)^3P_g$	0	0
$^3\Sigma^+$, $^3\Sigma^-(2)$, $^3\Pi(3)$, $^3\Delta(2)$, $^3\Phi$	$(3p^2)^1D_g + (2p^4)^3P_g$	6124	7597

[a] Ref 63.

TABLE 2: Spectroscopic Parameters of the Λ-S States of SiO

	T_e (cm^{-1})		r_e (Å)		ω_e (cm^{-1})	
state	theory	expt[a]	theory	expt[a]	theory	expt[a]
$X^1\Sigma^+$	0	0	1.521	1.5097	1216	1241.6
			1.61[b]		1015[b]	
			1.50[c]			
			1.496[e]		1248[e]	
			1.515[f]		1242[f]	
			1.519[g]		1241[g]	
			1.514[h]		1267[h]	
$a^3\Sigma^+$	33 568	33 630	1.708	1.70	821	790
	24 116[b]		1.86[b]		664[b]	
	37 827[c]		1.74[c]		671[d]	
	32 343[d]		1.70[d]			
$b^3\Pi$	34 337	33 845	1.586	1.5624	1012	1013.8
	30 730[b]		1.71[b]		805[b]	
	35 972[c]		1.60[c]		861[d]	
	35 327[d]		1.60[d]			
$d^3\Delta$	36 880	36 487	1.717	1.715	797	767
	30 972[b]		1.88[b]		625[b]	
	41 941[c]		1.76[c]		845[d]	
	35 085[d]		1.71[d]			
$e^3\Sigma^-$	37 848	38 309	1.738	1.726	785	748
	32 988[b]		1.90[b]		596[b]	
	43 473[c]		1.78[c]		803[d]	
	36 537[d]		1.73[d]			
$C\ ^1\Sigma^-$	37 920	38 624	1.743	1.727	725	740
	34 843[b]		1.96[b]		515[b]	
	44 925[c]		1.83[c]		735[d]	
	37 343[d]		1.77[d]			
			1.746[e]		703[e]	
$D^1\Delta$	38 955	38 823	1.744	1.729	732	730
	35 408[b]		1.98[b]		464[b]	
	46 457[c]		1.85[c]		708[d]	
	37 182[d]		1.79[d]			
$A^1\Pi$	43 863	42 835.4	1.650	1.6206	813	852.8
	38 634[b]		1.75[b]		676[b]	
	45 328[c]		1.64[c]		853[d]	
	39 360[d]		1.67[d]			
			1.644[e]		814[e]	
$E^1\Sigma^+$	52 965	52 860.9	1.755	1.73978	725	675.5
	48 151[d]		1.91[d]		567[d]	
			1.779[e]		620[e]	
$c^3\Sigma^+$	56 495	57 551.3	1.578	1.5561	828	949.1
$^5\Pi$	59 809		1.800		618	
	41 699[b]		2.19[b]			
$2^1\Pi$	61 850		1.705		687	
$g^3\Sigma^+$	67 077	68 091.4	1.535	1.52116	1176	
$2^3\Sigma^-$	73 445		1.659		794	
$^5\Sigma^-$	82 167		1.684		837	

[a] Ref 55. [b] Ref 27. [c] Predicted values in ref 27. [d] Ref 28. [e] SCF + CI in ref 29. [f] MCSCF−CI in ref 30. [g] CEPA-1 in ref 31. [h] CI−SD(s) in ref 32.

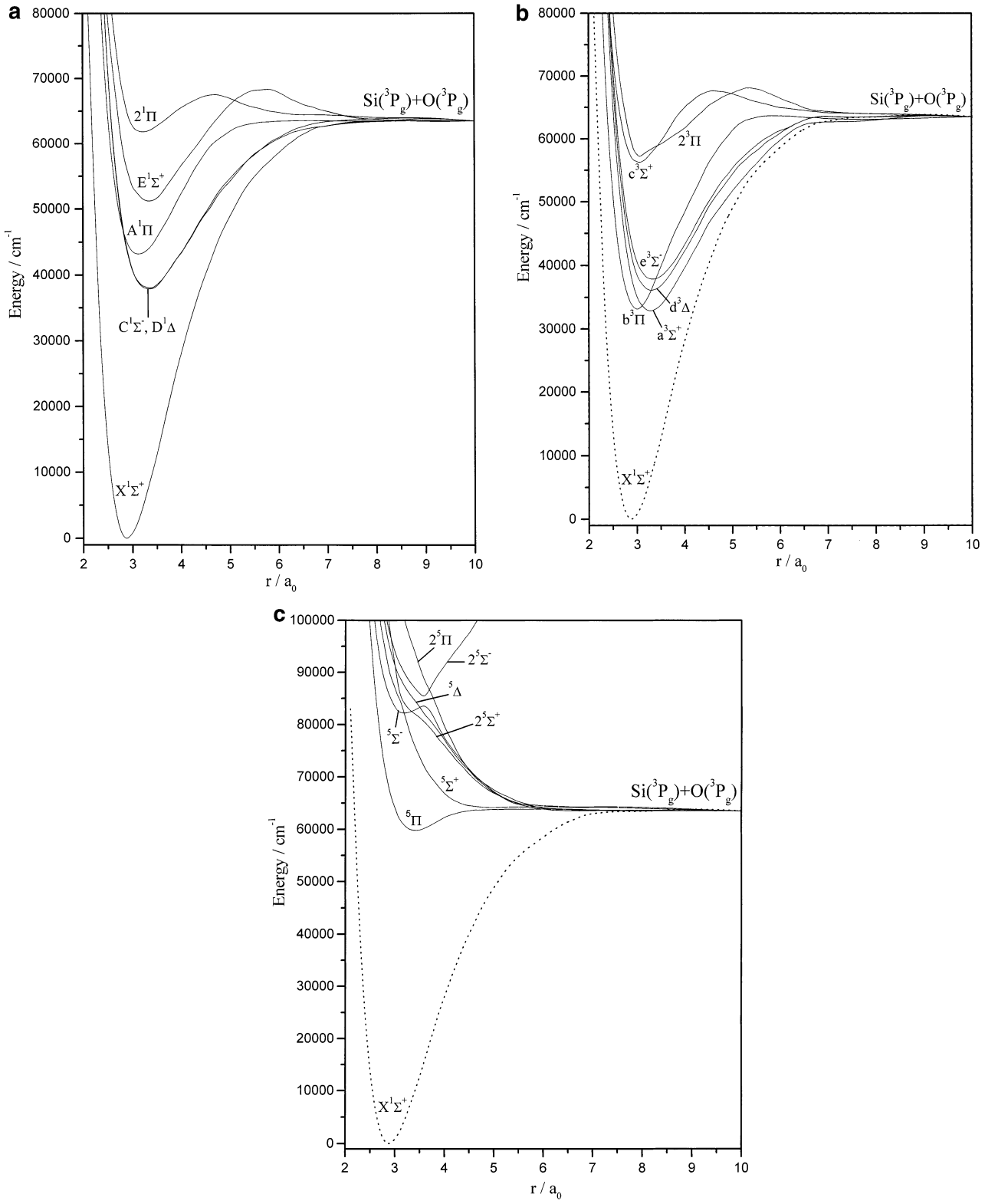

Figure 1. Computed potential energy curves of Λ-S states of SiO for (a) singlet, (b) triplet, and (c) quintet spin multiplicities.

(T_e, r_e, and ω_e) of 17 Λ-S states of SiO within 10 eV. Many of these states are experimentally observed. The results computed here are compared with the experimental and other theoretical data available so far. The ground state ($X^1\Sigma^+$) of SiO is dominated by a closed-shell $\sigma^2\pi^4$ (89%) configuration in which the σ orbital is a bonding type comprising s,p_z (Si) and p_z (O) atomic orbitals. The π MO is mainly localized on the $p_{x/y}$ atomic orbitals of the oxygen atom, but a weak bonding combination with $p_{x/y}$ (Si) is also noted. The computed ground state equilibrium bond length is 0.011 Å longer than the observed value of 1.5097 Å. The vibrational frequency of the ground state of SiO is calculated to be 1216 cm^{-1}, which agrees well with the experimental value of 1241.6 cm^{-1}. Earlier calculations of Heil and Schaefer[27] have reported somewhat different values. These authors have empirically predicted T_e, D_e, and r_e values of the low-lying states of SiO by using the difference between the calculated and the experimental values of the corresponding states of isovalent CO. Many other previously reported cor-

related calculations have given somewhat better r_e and ω_e values of the ground state molecule. Using the SCF + CI method, Langhoff and Arnold[29] have calculated the ground state r_e as 1.496 Å, which is shorter than the experimental value[33] of 1.5097 Å. However, their ω_e value of 1248 cm^{-1} is very close to the observed value of 1241.4 cm^{-1}. Both r_e and ω_e values of the ground state SiO obtained from MCSCF−CI calculations of Werner et al.[30] match excellently with the experimental values. The CEPA-1 calculations of Botschwina and Rosmus[31] have reported 1.519 Å and 1241 cm^{-1} as r_e and ω_e values for the ground state of the SiO molecule. The r_e value of the $X^1\Sigma^+$ state of SiO from CI−SD(s) calculations[32] is overestimated only by 0.005 Å, while the ω_e value is larger by 25 cm^{-1}.

Analogous to $a'^3\Sigma^+$ of the isovalent CO molecule, the $a^3\Sigma^+$ state is the first excited state of SiO. The MRDCI-estimated transition energy of the $a^3\Sigma^+$ state is 33 568 cm^{-1}, which matches nicely with the observed T_0 = 33 409 cm^{-1} obtained from the triplet−singlet intercombination $a^3\Sigma^+ \rightarrow X^1\Sigma^+$ emission band system in chemiluminescence of SiO.[13,20,22] The computed r_e and ω_e of $a^3\Sigma^+$ are 1.708 Å and 821 cm^{-1}, respectively. The predicted constants[54,55] are found to agree with our calculated values. The bond length of the $a^3\Sigma^+$ state, estimated from the potential energy curve of SiO using the Rydberg−Klein method, has been found to be 1.70 Å.[20] The $a^3\Sigma^+$ state is found to be strongly bound with a binding energy of 3.88 eV. As shown in Table 2, spectroscopic constants obtained in earlier calculations[27] have larger inaccuracies. The compositions of MRDCI wave functions show that the $a^3\Sigma^+$ state is described mainly by a singly excited configuration such as $\pi^3\pi^*$, where the π^* MO is weakly antibonding with its charge distribution more localized on the Si atom.

The same $\pi \rightarrow \pi^*$ excitation generates five other Λ-S states, which are denoted as $d^3\Delta$, $e^3\Sigma^-$, $C^1\Sigma^-$, $D^1\Delta$, and $E^1\Sigma^+$. All five states are strongly bound and dissociate into the lowest asymptote of SiO. The lowest four states are represented almost purely by a single configuration such as $\pi^3\pi^*$. On the other hand, the $E^1\Sigma^+$ state, which is the second root of the $^1\Sigma^+$ symmetry, has shown a configuration mixing with 62% contribution from $\pi^3\pi^*$. Three states such as $e^3\Sigma^-$, $C^1\Sigma^-$, and $D^1\Delta$ are nearly degenerate with their transition energies lying around 38 000 cm^{-1}, while the $d^3\Delta$ state lies below these states by about 2000 cm^{-1}. Field et al.[54] have investigated the perturbation of the A−X system and determined the spectroscopic constants of four perturbing states, namely, $C^1\Sigma^-$, $D^1\Delta$, $e^3\Sigma^-$, and $d^3\Delta$. The transition energy of the $d^3\Delta$ state computed here is 36 880 cm^{-1}, which agrees well with the experimental value of 36 487 cm^{-1}. The agreement between the calculated and the experimental values of r_e and ω_e of the $d^3\Delta$ state is also reasonably good. Energetically, the $e^3\Sigma^-$ state lies 968 cm^{-1} above $d^3\Delta$. The transition energy of $e^3\Sigma^-$, estimated from the experimental data, is reported to be 38 309 cm^{-1}, while the T_e value calculated in the present study is underestimated by 460 cm^{-1}. The MRDCI-estimated r_e of the $e^3\Sigma^-$ state is 0.012 Å longer than the experimental value of 1.726 Å, while the calculated ω_e is larger than the observed value by 37 cm^{-1}. The spin−orbit components of $e^3\Sigma^-$ are expected to undergo weak spin forbidden transitions to the ground state. The spectroscopic constants of the nearly degenerate $C^1\Sigma^-$ and $D^1\Delta$ states are very similar. Experimentally, the energy separation between these two states is only 200 cm^{-1}, while the present calculations show a separation of about 1000 cm^{-1}. However, the computed r_e and ω_e values of both of these states are found to agree well with the experimentally determined values as shown in Table 2. The r_e and ω_e values of the $C^1\Sigma^-$ state calculated from the SCF + CI study of Langhoff and Arnold[29] agree well with our results. In general, transition energies of all low-lying states of SiO calculated directly by Heil and Schaefer[27] are found to be much lower, but the positions of these states predicted empirically by the same authors are in better agreement. The vibrational frequencies calculated by these authors are also consistently much smaller than the experimental values. On the other hand, the molecular parameters of the low-lying excited states of SiO computed by Oddershede and Elander[28] using the self-consistent polarization propagator approximation, are more accurate.

The $b^3\Pi$ state lies very close to the first excited $a^3\Sigma^+$ state of the SiO molecule. The $b^3\Pi-X^1\Sigma^+$ transition, which is analogous to the spin forbidden Cameron band of CO, has been observed in the emission spectrum by many authors.[12,13,20] The calculated transition energy of the $b^3\Pi$ state of SiO is about 34 337 cm^{-1}, which is only 400 cm^{-1} above the observed T_0. The computed r_e and ω_e are also found to be in excellent agreement with the experimental values of 1.5624 Å and 1013.8 cm^{-1}, respectively.[55] It would be interesting to study how much intensity is being carried through such spin forbidden transitions. It may be mentioned here that the $b^3\Pi$ state is strongly bound with an estimated binding energy of 3.7 eV. The MRDCI wave functions show that the $b^3\Pi$ state is represented predominantly by the $\sigma\pi^4\pi^*$ (c^2 = 0.85) configuration. The same $\sigma \rightarrow \pi^*$ excitation generates the singlet counterpart of $b^3\Pi$, and it is denoted as $A^1\Pi$. The $A^1\Pi-X^1\Sigma^+$ band system is widely known for SiO, SiS, SnO, GeO, and other isovalent molecules. In Table 2, the spectroscopic constants of the $A^1\Pi$ state are compared with the observed and other theoretical values. In the present calculations, the transition energy of $A^1\Pi$ is overestimated by 1000 cm^{-1}. Transition energies obtained by Heil and Schaefer[27] as well as by Oddershede and Elander[28] are found to be too low. However, the predicted T_e and r_e reported by Heil and Schaefer[27] agree well with the observed data. The MRDCI-estimated equilibrium bond length of the $A^1\Pi$ state of SiO is 1.65 Å as compared to the experimental value of 1.6206 Å, while the calculated ω_e is smaller than the observed value by about 40 cm^{-1}. Earlier SCF + CI calculations[29] show a better agreement of r_e and ω_e for the $A^1\Pi$ state of the SiO molecule. It is expected that the A−X transition would be very strong in intensity. The potential energy curve of the A state is very smooth and dissociates into the lowest asymptote. The dissociation energy of $A^1\Pi$ computed from the potential energy curve is found to be 2.56 eV, which is in good agreement with the observed value of 2.87 ± 0.3 eV.[55,56]

The next electronic state, which is spectroscopically important, is $E^1\Sigma^+$. This state would, therefore, undergo a strong transition to the ground state of the same symmetry. For all isovalent molecules such as SiO, SiS, SiSe, GeO, SnO, etc., the E−X band is well-observed. The T_e value of the $E^1\Sigma^+$ state of SiO obtained in the E−X emission is 52 860.9 cm^{-1} as compared to the MRDCI-estimated value of 52 965 cm^{-1}. As seen in Figure 1a, the $E^1\Sigma^+$ state is reasonably strongly bound with a binding energy of 1.36 eV. The computed r_e and ω_e of the state also agree well with the experimentally derived values reported in Table 2. The composition of CI wave functions shows a multiconfiguration feature of the $E^1\Sigma^+$ state. However, in the equilibrium region of the potential energy curve, the state is dominantly represented by the $\pi^3\pi^*$ configuration ($c^2 \sim 0.6$). The closed shell (π^4) and other excited configurations contribute to a smaller extent. The fact that the potential curve of the $E^1\Sigma^+$ state dissociates adiabatically to the ground state atoms over a potential barrier near 5−5.5 a_0 is also noted by Langhoff and

Arnold[29] in their CI calculations. The r_e and ω_e of the $E^1\Sigma^+$ state calculated here are found to be reasonably accurate. Langhoff and Arnold[29] have calculated a somewhat larger r_e for the $E^1\Sigma^+$ state, while its ω_e is underestimated by about 56 cm^{-1}. The transition probabilities of the E−X transition will be of great importance in the present context. The radiative lifetimes of the $E^1\Sigma^+$ state at lower vibrational levels have been estimated by Elander and Smith.[57]

Potential energy curves of three more states, namely, $c^3\Sigma^+$, $2^3\Pi$, and $2^1\Pi$, which dissociate into the lowest asymptote, are shown in Figure 1a,b. A strong band system, $^3\Sigma^+-^3\Pi$ in the region of 4200−4300 Å, has been observed in the chemiluminescent flame spectrum of SiO.[8,11,21] The excited $^3\Sigma^+$ state is denoted here as $c^3\Sigma^+$, and its observed T_e is 57 551.3 cm^{-1}, which is larger than the calculated value by about 1000 cm^{-1}. The computed r_e of the $c^3\Sigma^+$ state is overestimated by ∼0.022 Å, while ω_e is underestimated by a larger extent. The potential energy curve of the $2^3\Pi$ state shows some avoided crossings with the minimum located around 57 900 cm^{-1}. The $2^1\Pi$ state is found to have a minimum at 1.705 Å with $T_e = 61\,850$ cm^{-1} and $\omega_e = 687$ cm^{-1}. A broad maximum around 4.5 a_0 indicates the presence of avoided crossings. No state of the $^1\Pi$ symmetry has been reported so far in this energy range. The $G^1\Pi \leftarrow X$ absorption band has been assigned[18,19] at $\nu_{00} = 69\,483$ cm^{-1}. However, the existence of the $G^1\Pi$ state cannot be confirmed in this study.

Among other low-lying states reported here, the $^5\Pi$ state lies at $T_e = 59\,809$ cm^{-1}. The estimated r_e and ω_e of this state are 1.80 Å and 618 cm^{-1}, respectively. The $^5\Pi$ state is weakly bound (binding energy ∼0.5 eV) dissociating into the lowest asymptote. Heil and Schaefer[27] have obtained somewhat different molecular parameters as tabulated in Table 2. The $^5\Pi$ state is found to be dominated by a single configuration such as $\sigma\pi^3\pi^{*2}$. Experimentally, there is no evidence of the $^5\Pi$ state. Singh et al.[11] have identified a triple-headed and violet-degraded band of SiO at 2970 Å and assigned it to a $d^3\Sigma^+-a^3\Pi$ transition. The upper state has been located 33 640 cm^{-1} above the $a^3\Pi$ state. Later on, the lower state is denoted as $b^3\Pi$, while the final state has been redesignated as $g^3\Sigma^+$. In the present study, there exists a bound state of the $^3\Sigma^+$ symmetry with $T_e = 67\,077$ cm^{-1}, which is somewhat lower than T_e of 68 091.4 cm^{-1} obtained from the above-mentioned high-resolution spectrum. The $g^3\Sigma^+$ state has some Rydberg components, and the Si−O bond at equilibrium is considerably short. The calculated $r_e = 1.535$ Å compares well with the experimentally determined value of 1.52116 Å. The computed ω_e is found to be comparable with that of the ground state. Although there is no experimental data, the $2^3\Sigma^-$ state is located around 73 445 cm^{-1} with $r_e = 1.659$ Å and $\omega_e = 794$ cm^{-1}. As seen in Figure 1c, the quintet states dissociating into the lowest asymptote are mostly repulsive. The $^5\Sigma^-$ state undergoes a strong avoided crossing with its higher counterpart. The minimum of $^5\Sigma^-$ is tentatively located around 82 167 cm^{-1}, and the estimated r_e and ω_e are 1.684 Å and 837 cm^{-1}, respectively.

The ground state dissociation energy (D_e) of SiO has been estimated from the MRDCI energies at very long distances ($r > 15$ a_0). There are several thermochemical D_0^0 values available for SiO. The calculated D_e is found to be 7.87 eV, which compares well with the experimental values of 7.93 ± 0.13,[23] 8.18 ± 0.3,[56] and 8.36 eV.[58] The smallest discrepancy of about 0.3 eV may be considered to be within the limit of accuracy of the MRDCI methodology used here. However, the ground state D_e of 8.1 eV computed from the CI calculations by Langhoff and Arnold[29] has shown a better agreement with the experimental one. The computed dissociation energy of the $A^1\Pi$ state is 2.44 eV as compared to the observed values of 2.70[23] and 2.87 ± 0.3 eV[56] deduced from the $A \rightarrow X$ excitation energy. Although the basis sets employed here are considerably large, the discrepancy is mainly because of the use of the effective core potentials.

TABLE 3: Dissociation Relation between Ω States and Atomic States of SiO

Ω state	atomic state	relative energy[a] (cm^{-1})
0^+, 1, 2	$^3P_0 + {}^3P_2$	0
0^+, 0^-(2), 1(3), 2(2), 3	$^3P_1 + {}^3P_2$	77
0^-, 1	$^3P_0 + {}^3P_1$	158
0^+(3), 0^-(2), 1(4), 2(3), 3(2), 4	$^3P_2 + {}^3P_2$	223
0^+	$^3P_0 + {}^3P_0$	227
0^+(2), 0^-, 1(2), 2,	$^3P_1 + {}^3P_1$	235
0^-, 1	$^3P_1 + {}^3P_0$	304
0^+, 0^-(2), 1(3), 2(2), 3	$^3P_2 + {}^3P_1$	381
0^+, 1, 2	$^3P_2 + {}^3P_0$	450

[a] Ref 63.

TABLE 4: Spectroscopic Constants of Ω States of SiO

state	T_e (cm^{-1})	r_e (Å)	ω_e (cm^{-1})	composition at r_e
$X^1\Sigma^+_{0^+}$	0	1.522	1211	$X^1\Sigma^+$(0.99)
$a^3\Sigma^+_{0^-}$	33 601	1.707	807	$a^3\Sigma^+$(0.99)
$a^3\Sigma^+_1$	33 744	1.682	914	$a^3\Sigma^+$(0.99)
$b^3\Pi_{0^-}$	34 295	1.581	1006	$b^3\Pi$(0.99)
$b^3\Pi_{0^+}$	34 296	1.582	1007	$b^3\Pi$(0.99)
	33 874.8[a]			
$b^3\Pi_1$	34 349	1.582	1006	$b^3\Pi$(0.99)
	33 947.4[a]			
$b^3\Pi_2$	34 430	1.581	1007	$b^3\Pi$(0.99)
	34 018.5[a]			
$d^3\Delta_1$	36 676	1.723	799	$d^3\Delta$(0.75), $^3\Pi$(0.25)
$d^3\Delta_2$	36 724	1.722	800	$d^3\Delta$(0.99)
$d^3\Delta_3$	36 945	1.718	808	$d^3\Delta$(0.99)
$e^3\Sigma^-_{0^+}$	37 644	1.735	793	$e^3\Sigma^-$(0.99)
$e^3\Sigma^-_1$	37 749	1.731	771	$e^3\Sigma^-$(0.99)
$C^1\Sigma^-_{0^-}$	37 964	1.743	729	$C\ ^1\Sigma^-$(0.96), $^3\Pi$(0.037)
$D\ ^1\Delta_2$	38 990	1.748	728	$D^1\Delta$(0.99)
$A^1\Pi_1$	43 865	1.650	821	$A^1\Pi$(99)
$E^1\Sigma^+_{0^+}$	52 863	1.753	703	$E^1\Sigma^+$(0.99)
$^5\Pi_3$	59 690	1.798	615	$^5\Pi$(0.99)

[a] Ref 55.

Spin−Orbit Coupling and Low-Lying Ω States. All 18 Λ-S states, which dissociate into the lowest asymptote $Si(^3P_g) + O(^3P_g)$, are allowed to interact through the spin−orbit coupling. The $^3P_g + {}^3P_g$ level splits into nine asymptotes, which correlate with 50 Ω states of different symmetries as shown in Table 3. In general, the spin−orbit splittings are considerably small due to the lower mass of the molecule. Nine dissociation limits are spaced within only 450 cm^{-1}. Potential energy curves of bound Ω states are drawn in Figure 2a−d, while their estimated spectroscopic constants are tabulated in Table 4. As a result of very weak spin−orbit coupling, spectroscopic parameters do not change much. Two spin−orbit components of $a^3\Sigma^+$ are separated only by 143 cm^{-1}. The equilibrium bond length of $a^3\Sigma^+_1$ is shortened, while its ω_e is increased to a small extent. The $a^3\Sigma^+_1$ component is spectroscopically important because the spin forbidden $a^3\Sigma^+_1-X^1\Sigma^+_{0^+}$ band has been studied in chemiluminescent flame spectra[20,22] of the SiO molecule. The components of $b^3\Pi$ split in a regular order $b^3\Pi_{0^-} < b^3\Pi_{0^+} < b^3\Pi_1 < b^3\Pi_2$. The largest spin−orbit splitting is less than 150 cm^{-1}. The spin forbidden $b^3\Pi_r-X^1\Sigma^+$ transition has been observed in emission.[12] The observed transition energies of $b^3\Pi_1$ and $b^3\Pi_1$ are 33 874.8 and 33 947.4 cm^{-1}, respectively, in good

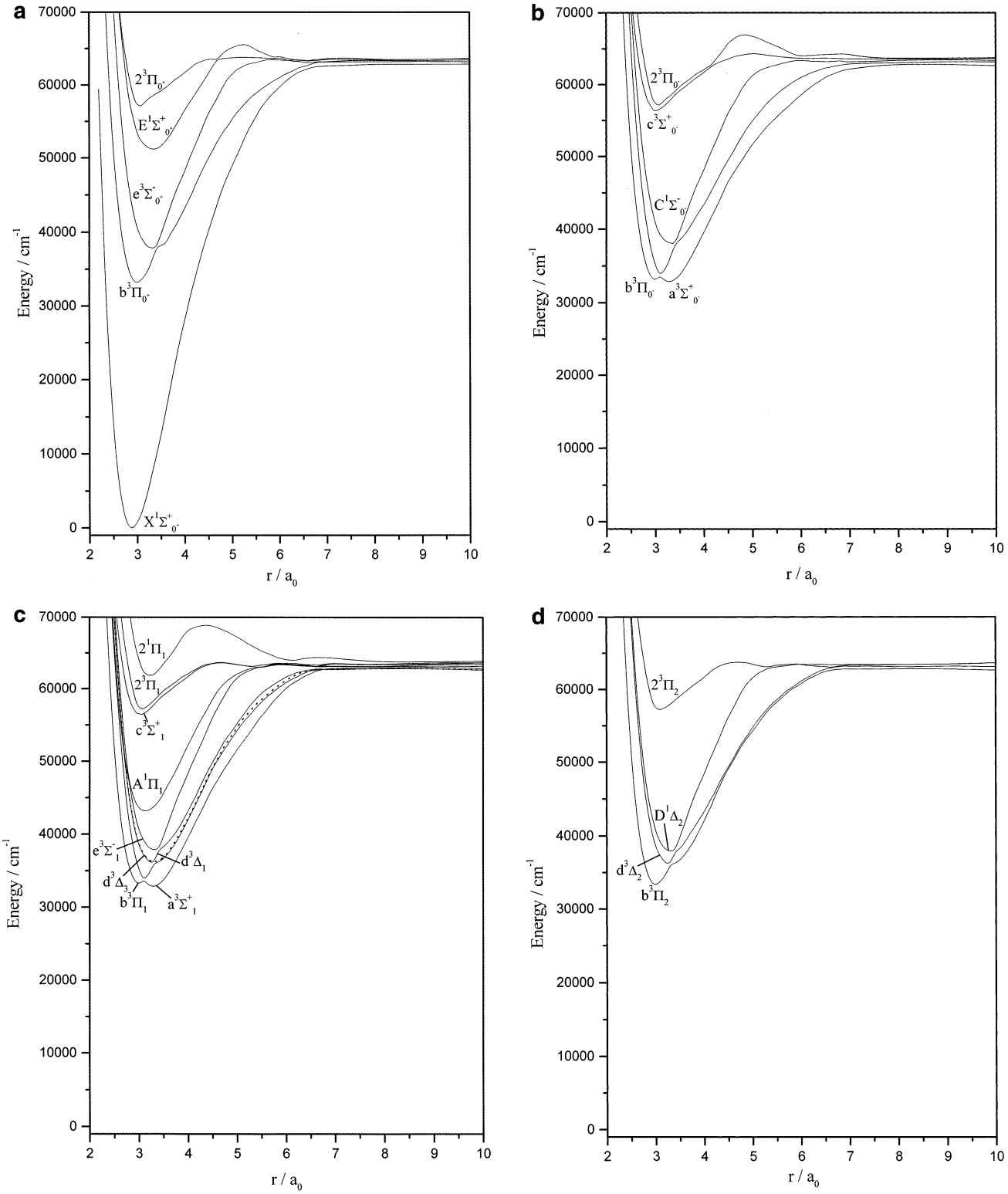

Figure 2. Computed potential energy curves of Ω states of SnO for (a) $\Omega = 0^+$, (b) $\Omega = 0^-$, (c) $\Omega = 1$ and 3, and (d) $\Omega = 2$.

agreement with the calculated values (see Table 4). The avoided crossings of both $b^3\Pi_{0^-}$ and $b^3\Pi_1$ with the corresponding components of $a^3\Sigma^+$ are nicely demonstrated in Figure 2b,c. It may be mentioned that $b^3\Pi_1-X^1\Sigma^+_{0^+}$ and $b^3\Pi_{0^+}-X^1\Sigma^+_{0^+}$ transitions are analogous to the strongest spin forbidden $a^3\Pi-X^1\Sigma^+$ Cameron band of the isovalent CO molecule. The $d^3\Delta$ state also splits in a regular order $d^3\Delta_1 < d^3\Delta_2 < d^3\Delta_3$ with a largest separation of 269 cm^{-1}. Spectroscopic parameters of these components do not change significantly. Several sharp avoided crossings are noted in the Franck−Condon region of the $d^3\Delta_1$ curve. At r_e, the coefficient of mixing of $d^3\Delta_1$ with the $b^3\Pi_1$ component is shown in Table 4. The $d^3\Delta_1$ component is suitable for its transition to the ground state. Both of the components ($\Omega = 0^+$ and 1) of $e^3\Sigma^-$ undergo allowed transitions to the ground state. The spin−orbit splitting of these two components is estimated to be only about 100 cm^{-1}. No significant changes take place for the spin−orbit components of singlet states such as $C^1\Sigma^-_{0^-}$, $D^1\Delta_2$, $A^1\Pi_1$, and $E^1\Sigma^+_{0^+}$. The $A^1\Pi_1-X^1\Sigma^+_{0^+}$ and

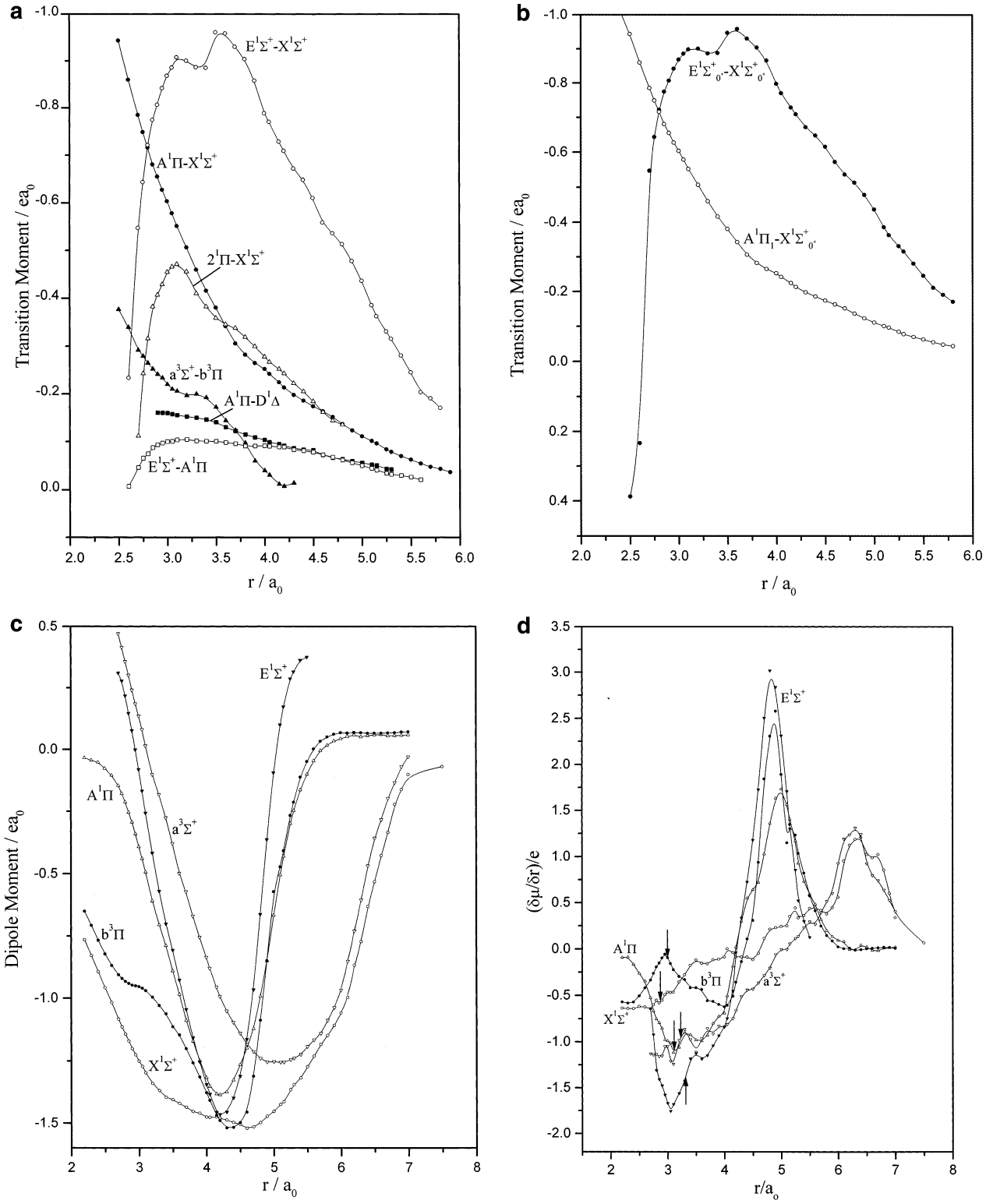

Figure 3. (a) Transition moment curves of six singlet−singlet and triplet−triplet transitions involving Λ-S states of SiO. (b) Transition moment curves of two transitions involving Ω components of SiO. (c) Dipole moment functions of $X^1\Sigma^+$, $b^3\Pi$, $A^1\Pi$, $a^3\Sigma^+$, and $E^1\Sigma^+$. (d) Dipole derivative functions of $X^1\Sigma^+$, $b^3\Pi$, $A^1\Pi$, $a^3\Sigma^+$, and $E^1\Sigma^+$ (arrows pointing toward the respective r_e values).

$E^1\Sigma^+_{0^+}-X^1\Sigma^+_{0^+}$ transitions studied by several authors are expected to be quite strong. In the next section, we shall discuss transition probabilities of these two transitions. The potential curve of the $^5\Pi_3$ component has been fitted, and the estimated transition energy is found to be 59 690 cm^{-1}, while its r_e and ω_e are 1.798 Å and 615 cm^{-1}, respectively. However, spectroscopically, the $^5\Pi_3$ component does not have much significance.

Transition Properties and Radiative Lifetimes of Upper States. Transition moments of several dipole-allowed and spin forbidden transitions are computed from the MRDCI energies and wave functions. In the absence of any spin−orbit interaction, three singlets, namely, $2^1\Pi$, $E^1\Sigma^+$, and $A^1\Pi$, are chosen for symmetry-allowed transitions to the lower singlets. The $c^3\Sigma^+ \rightarrow b^3\Pi$ transition is also considered in this study. The transition moments of six transitions are plotted in Figure 3a as a function

TABLE 5: Radiative Lifetimes (s) of Some Excited Singlet Λ-S States at Lowest Three Vibrational Levels of SiO[a]

	lifetime of the upper state			total lifetime of upper state at
transition	$\nu' = 0$	$\nu' = 1$	$\nu' = 2$	$\nu' = 0$
$A^1\Pi - X^1\Sigma^+$	28.9(−9)	28.7(−9)	28.6(−9)	
$A^1\Pi - D^1\Delta$	1.93(−4)	1.60(−4)	1.38(−4)	$\tau(A^1\Pi) = 28.9(-9)$
$E^1\Sigma^+ - X^1\Sigma^+$	7.10(−9)	6.89(−9)	6.95(−9)	
$E^1\Sigma^+ - A^1\Pi$	1.01(−4)	9.9(−5)	9.9(−5)	$\tau(E^1\Sigma^+) = 7.10(-9)$
$2^1\Pi - X^1\Sigma^+$	14.85(−9)	15.98(−9)	17.43(−9)	$\tau(2^1\Pi) = 14.85(-9)$
$2^3\Pi - b^3\Pi$	1.51(−7)	1.38(−7)	1.34(−7)	$\tau(2^3\Pi) = 1.51(-7)$
$c^3\Sigma^+ - b^3\Pi$	8.10(−7)	8.36(−7)	8.69(−7)	$\tau(c^3\Sigma^+) = 8.10(-7)$

[a] Values in the parentheses are the powers to the base 10.

of the bond length. In the Franck−Condon region, the transition moments of E−X and A−X transitions are considerably large. The transition moment curve of the E−X transition shows a hump between 3.0 and 4.0 a_0, while that of A−X is monotonically decreasing. The transition moment of the $2^1\Pi - X^1\Sigma^+$ transition has been found to give a maximum around $r = 3.1$ a_0. All three transitions A−X, E−X, and $2^1\Pi$−X are expected to be strong. The computed transition moments of other transitions are comparatively small. The estimated radiative lifetimes (partial and total) of the low-lying states of SiO are given in Table 5. The total radiative lifetime of $A^1\Pi$ at the lowest vibrational level ($\nu' = 0$) is found to be 28.9 ns, which compares well with the value of 31.6 ns obtained from the experimental potential energy curves. Smith and Liszt[59] have determined the radiative lifetime $\tau(A^1\Pi) = 9.6 \pm 1.0$ ns from the phase shift measurement. This value is about three times smaller than the calculated one. Oddershede and Elander[28] have estimated an average value of 49.5 ns as the calculated radiative lifetime of $A^1\Pi$ for the $A^1\Pi - X^1\Sigma^+$ transition in SiO. These authors have used the shapes of the experimental potential curves of $A^1\Pi$ and $X^1\Sigma^+$ carried out by Deutsch et al.[60] and Barrow and Stone.[17] The electronic oscillator strengths for the $A^1\Pi - X^1\Sigma^+$ transition in SiO have been determined from shock tube and laser beam studies.[55,61,62]

The present calculations show that the $A^1\Pi - D^1\Delta$ transition is considerably weak. The partial lifetime of $A^1\Pi$ for this transition is of the order of 10^{-4} s. This particular transition does not alter the total lifetime of the $A^1\Pi$ state. The $E^1\Sigma^+ - X^1\Sigma^+$ transition is found to be stronger than the A−X transition. The computed radiative lifetime of $E^1\Sigma^+$ at $\nu' = 0$ is only 7.1 ns. Elander and Smith[57] have determined the radiative lifetime for the $E^1\Sigma^+$ state by using the electron beam phase shift technique. The value reported from this experiment is 10.5 ns, which agrees well with the lifetime computed here. These authors have also calculated Franck−Condon factors and f values for bands of the $\nu' = 0$ progression and determined the r dependence of the transition moment. Another possible transition $E^1\Sigma^+ - A^1\Pi$ is weak, and the partial lifetime of $E^1\Sigma^+$ for this transition is found to be 1.01×10^{-4} s. The $2^1\Pi$ state may be a good candidate for its transition to the ground state. The computed transition probabilities predict the $2^1\Pi - X^1\Sigma^+$ transition to be quite strong. The radiative lifetime of the $2^1\Pi$ state at $\nu' = 0$ is calculated to be 14.85 ns. However, no experimental data are available for comparison.

It has been mentioned earlier that several spin forbidden transitions such as $a^3\Sigma^+ - X^1\Sigma^+$, $b^3\Pi - X^1\Sigma^+$, and $e^3\Sigma^- - X^1\Sigma^+$ are observed in the chemiluminescent flame spectra of the SiO molecule. The transition moments of $a^3\Sigma_1^+ - X^1\Sigma_{0^+}^+$ are negligibly small so that the transition is found to be very weak. Transition probabilities of $b^3\Pi_{0^+} - X^1\Sigma_{0^+}^+$ and $b^3\Pi_1 - X^1\Sigma_{0^+}^+$, which are analogous to the Cameron band of CO, are also calculated in the present study. The partial radiative lifetimes of $b^3\Pi_{0^+}$ and $b^3\Pi_1$ components at the lowest vibrational level are 9.72 and 1.15 ms, respectively (see Table 6). Transitions from both the components of $e^3\Sigma^-$ to the ground state are somewhat stronger. The partial lifetimes of $e^3\Sigma_{0^+}^-$ and $e^3\Sigma_1^-$ components are estimated to be 0.13 and 0.68 ms, respectively. The $^3\Delta_1$ component also undergoes a weak spin forbidden transition to the ground state component. The computed radiative lifetime of the $d^3\Delta_1 - X^1\Sigma_{0^+}^+$ transition at the lowest vibrational level of the upper state is 3.2 ms. Both the strong transitions $A^1\Pi - X^1\Sigma^+$ and $E^1\Sigma^+ - X^1\Sigma^+$ remain unperturbed due to the spin−orbit coupling. As seen in Table 6, the lifetimes of $A^1\Pi_1$ and $E^1\Sigma_{0^+}^+$ components do not differ much from the values in their Λ-S states. The shapes of the transition moment curves of $A^1\Pi_1 - X^1\Sigma_{0^+}^+$ and $E^1\Sigma_{0^+}^+ - X^1\Sigma_{0^+}^+$, as shown in Figure 3b, are not altered due to the spin−orbit coupling.

TABLE 6: Radiative Lifetimes (s) of Some Excited Ω States at Lowest Three Vibrational Levels of SiO[a]

	lifetime of the upper state			total lifetime of upper state at
transition	$\nu' = 0$	$\nu' = 1$	$\nu' = 2$	$\nu' = 0$
$A^1\Pi_1 - X^1\Sigma_{0^+}^+$	28.83(−9)	28.69(−9)	28.59(−9)	$\tau(A^1\Pi_1) = 28.89(-9)$
$E^1\Sigma_{0^+}^+ - X^1\Sigma_{0^+}^+$	7.42(−9)	7.14(−9)	7.27(−9)	$\tau(E^1\Sigma_{0^+}^+) = 7.42(-9)$
$b^3\Pi_{0^+} - X^1\Sigma_{0^+}^+$	9.72(−3)	7.90(−3)	6.39(−3)	$\tau(b^3\Pi_{0^+}) = 9.72(-3)$
$b^3\Pi_1 - X^1\Sigma_{0^+}^+$	1.15(−3)	1.15(−3)	1.13(−3)	$\tau(b^3\Pi_1) = 1.15(-3)$
$e^3\Sigma_{0^+}^- - X^1\Sigma_{0^+}^+$	6.76(−4)	7.07(−4)	7.50(−4)	$\tau(e^3\Sigma_{0^+}^+) = 6.76(-4)$
$e^3\Sigma_1^- - X^1\Sigma_{0^+}^+$	1.26(−4)	1.28(−4)	1.33(−4)	$\tau(e^3\Sigma_1^-) = 1.26(-4)$
$d^3\Delta_1 - X^1\Sigma_{0^+}^+$	3.20(−3)	4.65(−3)	9.56(−3)	$\tau(d^3\Delta_1) = 3.20(-3)$

[a] Values in the parentheses are the powers to the base 10.

TABLE 7: Calculated Dipole Moments and Dipole Derivatives of the Low-Lying States of SiO

	μ_e (D)		$\partial\mu/\partial r\|_{r_e}$ (D/Å)	
state	expt[a]	calcd	expt[b]	calcd
$X^1\Sigma^+$	−3.0882	−3.03	−2.22	−2.72
		−3.677[b]		−5.06[b]
		−2.963[c]		
		−2.993[d]		
		−3.057[e]		
		−3.195[f]		
		−2.846[g]		
		−3.044[h]		−2.944[h]
		−3.01[i]		
$a^3\Sigma^+$		−0.30		−4.71
$b^3\Pi$		−2.43		−0.47
$A^1\Pi$		−1.28		−5.28
$E^1\Sigma^+$		−1.48		−6.66

[a] Ref 33. [b] Ref 25. [c] MCSCF−CI in ref 29. [d] MCSCF in ref 30. [e] CEPA-1 in ref 31. [f] CI-SD in ref 32. [g] Ref 34. [h] (433)ACPF in ref 35. [i] Ref 36.

In Figure 3c, we have shown the dipole moments of the SiO molecule in $X^1\Sigma^+$, $b^3\Pi$, $a^3\Sigma^+$, $A^1\Pi$, and $E^1\Sigma^+$ electronic states as a function of the internuclear distance. The negative sign of the dipole moment indicates the $Si^+ - O^-$ polarity. All of the dipole moment curves tend to zero in the very large bond length region ($r > 20$ a_0) indicating that the atomic transitions are dipole forbidden and the atoms are neutral. At r_e, the ground state dipole moment of SiO is calculated to be −3.03 D, which agrees well with the experimental value[25] of −3.0882 D determined from the molecular beam electric resonance spectra of the molecule. Figure 3c shows that the ground state dipole moment maximizes (−1.521 ea_0) at $r = 4.6$ a_0. Dipole moment curves of other states show an identical pattern. In Table 7, we have compared different theoretical and experimental electric dipole moments (μ_e) and dipole derivatives ($\partial\mu/\partial r|_{r_e}$) of the

ground and a few low-lying states of SiO. Many calculations at different levels of the electron correlation have reported the ground state μ_e. It may be noted that the calculated μ_e values are found to be smaller than the observed value. The dipole moments of the excited states such as $A^1\Pi$, $E^1\Sigma^+$, $a^3\Sigma^+$, and $b^3\Pi$ at their respective equilibrium bond lengths are found to be smaller than the ground state μ_e. These excited states are mainly generated by either $\sigma^*\pi^*$ or $\pi^*\pi^*$ excitations, which tend to move the electronic charge in the direction of Si, thereby lowering their dipole moment from the ground state value. The dipole derivatives $(\partial\mu/\partial r)$ at r_e have been calculated from the dipole moment functions. Figure 3d shows the dipole derivatives of five states as a function of the bond length. The calculated $\partial\mu/\partial r|r_e$ value for the ground state is found to agree well with the experimental value of -2.22 D/Å. The value obtained by Langhoff and Bauschlicher[35] in (433)ACPF calculations is about -2.944 D/Å. However, the calculated value reported in the work of Raymonda et al.[25] is more than twice the experimental one.

IV. Conclusion

Using RECP-based MRDCI method, spectroscopic properties of low-lying electronic states of SiO have been calculated. In general, the computed spectroscopic parameters agree well with the experimental data. The ground state bond length of SiO is longer than the observed value by 0.011 Å, while its vibrational frequency differs by 26 cm^{-1}. For excited states such as $A^1\Pi$, $c^3\Sigma^+$, and $g^3\Sigma^+$, the discrepancies between the experimental and the computed transition energies are about 1000 cm^{-1}, while for other states such discrepancies are much less. The $a^3\Sigma^+$ and $b^3\Pi$ states are nearly degenerate but with a notable difference in bond lengths between them. The computed bond lengths of the observed states are, in general, 0.01−0.02 Å longer than the experimentally determined values. The ground state dissociation energy of the SiO molecule calculated here is smaller than the observed value by 0.3 eV within the limit of accuracy of the MRDCI method. The spin−orbit coupling does not change the spectroscopic parameters much. Besides some sharp avoided crossings, potential energy curves do not change their shapes. Transitions from $A^1\Pi$, $E^1\Sigma^+$, and $2^1\Pi$ states to the ground state are found to be highly probable. Two triplet−triplet transitions, namely, $2^3\Pi-b^3\Pi$ and $c^3\Sigma^+-b^3\Pi$, are also strong. The estimated radiative lifetimes of $A^1\Pi$ and $E^1\Sigma^+$ compare well with the experimentally determined values. Several spin forbidden transitions such as $b^3\Pi_{0^+}-X$, $e^3\Sigma^-_{0^+}-X$, $b^3\Pi_1-X$, $e^3\Sigma^-_1-X$, etc. are expected to be weak in intensity. The radiative partial lifetimes of these components are of the order of milliseconds. The computed dipole moment (μ_e) and its first derivative $(\partial\mu/\partial r|r_e)$ for the ground state of SiO agree well with the experimentally determined values.

Acknowledgment. The financial support received from the CSIR, Government of India through the scheme 1(1759)/02/EMR-II is gratefully acknowledged. We thank Prof. Dr. R. J. Buenker, Germany, for the CI codes. S.C. thanks CSIR for the award of a Junior Research Fellowship.

References and Notes

(1) Jevons, W. *Proc. R. Soc. London* **1924**, *106*, 174.
(2) Cameron, W. H. B. *Philos. Mag.* **1927**, *3*, 110.
(3) Saper, P. G. *Phys. Rev.* **1932**, *42*, 498.
(4) McGregor, A. T.; Nicholls, R. W.; Jamain, W. R. *Can. J. Phys.* **1961**, *39*, 1215.
(5) Rowlinson, H. C.; Barrow, R. F. *J. Chem. Phys.* **1953**, *21*, 378.
(6) Barrow, R. F.; Rowlinson, H. C. *Proc. R. Soc. London* **1954**, *A224*, 374.
(7) Verma, R. D.; Mulliken, R. S. *Can. J. Phys.* **1961**, *39*, 908.
(8) Nagaraj, S.; Verma, R. D. *Can. J. Phys.* **1970**, *48*, 1436.
(9) Nair, K. P. R.; Singh, R. B.; Rai, D. K. *J. Chem. Phys.* **1965**, *43*, 3570.
(10) Cornet, R.; Dubois, I. *Can. J. Phys.* **1972**, *50*, 630.
(11) Singh, M.; Bredohl, H.; Remy, F.; Dubois, I. *Can. J. Phys.* **1974**, *52*, 569.
(12) Bredohl, H.; Cornet, R.; Dubois, I.; Remy, F. *J. Phys. B: At., Mol. Phys.* **1974**, *7*, L66.
(13) Hager, G.; Wilson, L. E.; Hadley, S. G. *Chem. Phys. Lett.* **1974**, *27*, 439.
(14) Verma, R. D.; Shanker, R. *J. Mol. Spectrosc.* **1976**, *63*, 553.
(15) Cornet, R.; Dubois, I.; Gerkens, M.; Tripnaux, E. *Bull. Soc. R. Sci. Liège* **1972**, *41*, 183.
(16) Bredohl, H.; Cornet, R.; Dubois, I.; Remy, F. *Can. J. Phys.* **1973**, *51*, 2332.
(17) Barrow, R. F.; Stone, T. G. *J. Phys. B: At., Mol. Phys.* **1975**, *8*, L13.
(18) Lagerqvist, A.; Renhorn, I.; Elander, N. *J. Mol. Spectrosc.* **1973**, *46*, 285.
(19) Lagerqvist, A.; Renhorn, I. *J. Mol. Spectrosc.* **1974**, *49*, 157.
(20) Hager, G.; Harris, R.; Hadley, S. G. *J. Chem. Phys.* **1975**, *63*, 2810.
(21) Shanker, R.; Linton, C.; Verma, R. D. *J. Mol. Spectrosc.* **1976**, *60*, 197.
(22) Linton, C.; Capelle, G. A. *J. Mol. Spectrosc.* **1977**, *66*, 62.
(23) Hildenbrand, D. L.; Murad, E. *J. Chem. Phys.* **1969**, *51*, 807.
(24) Hildenbrand, D. L.; Murad, E. *J. Chem. Phys.* **1974**, *61*, 1232.
(25) Raymonda, J. W.; Muenter, J. S.; Klemperer, W. A. *J. Chem. Phys.* **1970**, *52*, 3458.
(26) McLean, A. D.; Yoshimine, M. *IBM J. Res. Dev. Suppl.* **1968**, *12*, 206.
(27) Heil, T. G.; Schaefer, H. F., III. *J. Chem. Phys.* **1972**, *56*, 958.
(28) Oddershede, J.; Elander, N. *J. Chem. Phys.* **1976**, *65*, 3495.
(29) Langhoff, S. R.; Arnold, J. O. *J. Chem. Phys.* **1979**, *70*, 852.
(30) Werner, H.-J.; Rosmus, P.; Grimm, M. *Chem. Phys.* **1982**, *73*, 169.
(31) Botschwina, P.; Rosmus, P. *J. Chem. Phys.* **1985**, *82*, 1420.
(32) Peterson, K. A.; Claude Woods, R. *J. Chem. Phys.* **1990**, *92*, 6061.
(33) Tipping, R. H.; Chackerian, C., Jr. *J. Mol. Spectrosc.* **1981**, *88*, 352.
(34) Kellö, V.; Sadlej, A. J. *J. Chem. Phys.* **1993**, *98*, 1345.
(35) Langhoff, S. R.; Bauschlicher, C. W., Jr. *Chem. Phys. Lett.* **1993**, *211*, 305.
(36) Maroulis, G.; Makris, C.; Xenides, D.; Karamanis, P. *Mol. Phys.* **2000**, *98*, 481.
(37) Robbe, J. M.; Lefebvre-Brien, H.; Gottscho, R. A. *J. Mol. Spectrosc.* **1981**, *85*, 215.
(38) Dutta, A.; Chattopadhyaya, S.; Das, K. K. *J. Phys. Chem.* **2001**, *A105*, 3232.
(39) Manna, B.; Das, K. K. *J. Phys. Chem.* **1998**, *A102*, 214.
(40) Dutta, A.; Manna, B.; Das, K. K. *Ind. J. Chem.* **2000**, *39A*, 163.
(41) Chattopadhyaya, S.; Chattopadhyay, A.; Das, K. K. *J. Phys. Chem.* **2002**, *A106*, 833.
(42) Balasubramanian, K. *Relativistic Effects in Chemistry Part A. Theory and Techniques*; Wiley-Interscience: New York, 1997.
(43) Balasubramanian, K. *Relativistic Effects in Chemistry Part B. Applications to Molecules and Clusters*; Wiley-Interscience: New York, 1997.
(44) Pacios, L. F.; Christiansen, P. A. *J. Chem. Phys.* **1985**, *82*, 2664.
(45) Matos, J. M. O.; Kellö, V.; Ross, B. O.; Sadlej, A. J. *J. Chem. Phys.* **1988**, *89*, 423.
(46) Buenker, R. J.; Peyerimhoff, S. D. *Theor. Chim. Acta* **1974**, *35*, 33.
(47) Buenker, R. J.; Peyerimhoff, S. D. *Theor. Chim. Acta* **1975**, *39*, 217.
(48) Buenker, R. J. *Int. J. Quantum Chem.* **1986**, *29*, 435.
(49) Buenker, R. J. In *Proceedings of the Workshop on Quantum Chemistry and Molecular Physics*; Burton, P., Ed.; University Wollongong: Wollongong, Australia, 1980.
(50) Buenker, R. J. In *Studies in Physical and Theoretical Chemistry*; Carbó, R., Ed.; Elsevier: Amsterdam, The Netherlands, 1981; Vol. 21 (Current Aspects of Quantum Chemistry).
(51) Buenker, R. J.; Phillips, R. A. *J. Mol. Struct. (THEOCHEM)* **1985**, *123*, 291.
(52) Davidson, E. R. In *The World of Quantum Chemistry*; Daudel, R., Pullman, B., Ed.; Reidel: Dordrecht, The Netherlands, 1974.
(53) Hirsch, G.; Bruna, P. J.; Peyerimhoff, S. D.; Buenker, R. J. *Chem. Phys. Lett.* **1977**, *52*, 442.
(54) Field, R. W.; Lagerqvist, A.; Renhorn, I. *J. Chem. Phys.* **1977**, *66*, 868.
(55) Huber, K. P.; Herzberg, G. In *Molecular Spectra and Molecular Structure*; Van Nostrand Reinhold: Princeton, NJ, 1979; Vol. 4 (Constants of Diatomic Molecules).

(56) Gaydon, A. G. *Dissociation Energies and Spectra of Diatomic Molecules*; Chapman and Hall: London, 1968.
(57) Elander, N.; Smith, W. H. *Astrophys. J.* **1973**, *184*, 311.
(58) Brewer, L.; Rosenblatt, G. M. *Advances in High-Temperature Chemistry*; Academic: New York, 1969; Vol. 2.
(59) Smith, W. H.; Liszt, H. S. *J. Quant. Spectrosc. Radiat. Transfer* **1972**, *12*, 505.
(60) Deutsch, J. L.; Deutsch, E. W.; Elander, N.; Lagerqvist, A. *Phys. Scr.* **1975**, *12*, 248.
(61) Main, R. P.; Morsell, A. L.; Hooker, W. J. *J. Quant. Spectrosc. Radiat. Transfer* **1968**, *8*, 1527.
(62) Hooker, W. J.; Main, R. P. *Physica* **1969**, *41*, 35.
(63) Moore, C. E. *Tables of Atomic Energy Levels*; U.S. National Bureau of Standards: Washington, DC, 1971; Vols. I−III.